EPJ Web of Conferences **26**, 04037 (2012)
DOI: 10.1051/epjconf/20122604037

Response of split Hopkinson bar apparatus signal to end-surface damage, *numerical and experimental studies*

A. Bouamoul and M. Bolduc

Defence Research and Development Canada, 2459 Pie-XI North, Quebec, QC, Canada, G3J 1X5

Abstract. A Split Hopkinson bar apparatus is a widely used method to obtain material properties at high strain rates. These properties are essential in the development of new materials as well as their associated constitutive models. During routine tests, the surfaces of the bars at the specimen/bars interface were damaged. To check if the damage influenced the signal response, control tests were done using the well characterized Al 6061-T6. Results showed that artefacts were added to the signal. This paper presents the experimental and numerical approaches developed to understand the effects of surface damage. The approach used consists of introducing series of known gaps between input and output bar to simulate a variation of surface damage. The numerical simulations, performed using a hydrocode, were done to confirm that signal response could not be associated with other several types of error in the system.

1 Introduction

Under high dynamic loading conditions, material responses are different from those in quasi-static regime. Most published data are mainly based on quasi-static tests in which the material deforms statically at an average strain rate of about 10^{-1} s^{-1} or under. During a ballistic impact or under blast loading conditions, the strain rate could exceed, in some cases, 10^5 s^{-1}. To obtain material properties at high strain rates, a dynamic test method is required. The split Hopkinson pressure bar (SHPB) technique is a common method used for determining these dynamic properties. The basic method was first introduced in 1949 by Kolsky [1]. However, many laboratories are now using this technique with modifications that provide different loading conditions. A variety of different data acquisition systems are also used. At Defense Research and Development Canada (DRDC) this technique is used in the development of new materials especially, design for high dynamic loading condition such as armor to defeat high velocity impact and blast loading. Another application where split Hopkinson pressure bar apparatus is widely used at our facility is material characterization for constitutive material models.

During a test series, the surfaces of the SHPB bars at the sample/bars interface were damaged. To verify if the damage might influence the signal response, control tests were performed using the well characterized Al 6061-T6 material. This material was chosen because it was well documented and tested at our SHPB facility [2].

2 Split Hopkinson pressure bar

A conventional Hopkinson bar consists of a striker, an incident and a transmitted bars, a specimen, and a momentum trap. Figure 1 shows a basic Hopkinson bar test set-up where the specimen is sandwiched between the incident and transmitted bars. To simplify mathematical calculations, theses two bars are made from the same material.

In a split Hopkinson bar, when the striker hits the incident bar, a rectangular compression wave with a specific amplitude and length moves through the length of the incident bar. The compressive wave is a function of the velocity and shape of the striker. When the wave reaches the end of the incident bar, a fraction of it is transmitted to the specimen and a part is reflected. This is due to the mismatch in the cross-sectional area and acoustic impedance between the bars and the specimen. The wave transmitted by the specimen to the transmitted bar is a function of specimen material properties and impedance.

The use of one-dimensional wave propagation analysis helps to determine high strain rate stress-stain curves from measurements of strain gauges in the incident and transmitted bars [3,4]. Assuming that both the incident and transmitted bars are made from the same material, the relationship expressing the strain rate in the specimen is given by Equation (1). Whereas, the stress in the specimen can be calculated by dividing the force in the transmitted bar by the cross-sectional area of the specimen, as given in Equation (2).

$$\dot{\varepsilon}_{specimen} = \frac{2c\varepsilon_r}{l_s} \tag{1}$$

$$\sigma_{specimen}(t) = \frac{AE\varepsilon_t}{A_s} \tag{2}$$

In equations (1) and (2), c is the sound speed in the incident and transmitted bar, l_s is the instantaneous length of the specimen, ε_r and ε_t are respectively, the reflected and transmitted strains, A is the cross-sectional area of the incident and transmitted bars, E is the Young's modulus of the two bars, A_s is the cross-sectional area of the specimen, $\dot{\varepsilon}_{specimen}$ and $\sigma_{specimen}$ are the strain rate and stress in the specimen.

3 Experimental tests

A complete description of the DRDC Valcartier system can be found in Ref. [5]. In summary, the SHPB system

Report Documentation Page

Form Approved
OMB No. 0704-0188

1. REPORT DATE **2012**	2. REPORT TYPE	3. DATES COVERED **00-00-2012 to 00-00-2012**

4. TITLE AND SUBTITLE **Response of split Hopkinson bar apparatus signal to end-surface damage, numerical and experimental studies**	5a. CONTRACT NUMBER
	5b. GRANT NUMBER
	5c. PROGRAM ELEMENT NUMBER
6. AUTHOR(S)	5d. PROJECT NUMBER
	5e. TASK NUMBER
	5f. WORK UNIT NUMBER
7. PERFORMING ORGANIZATION NAME(S) AND ADDRESS(ES) **Defence R&D Canada - Valcartier,2459 Pie-XI Blvd North,Quebec (Quebec) G3J 1X5 Canada,**	8. PERFORMING ORGANIZATION REPORT NUMBER
9. SPONSORING/MONITORING AGENCY NAME(S) AND ADDRESS(ES)	10. SPONSOR/MONITOR'S ACRONYM(S)
	11. SPONSOR/MONITOR'S REPORT NUMBER(S)

12. DISTRIBUTION/AVAILABILITY STATEMENT
Approved for public release; distribution unlimited

13. SUPPLEMENTARY NOTES

14. ABSTRACT

15. SUBJECT TERMS

16. SECURITY CLASSIFICATION OF:			17. LIMITATION OF ABSTRACT	18. NUMBER OF PAGES	19a. NAME OF RESPONSIBLE PERSON
a. REPORT **unclassified**	b. ABSTRACT **unclassified**	c. THIS PAGE **unclassified**	**Same as Report (SAR)**	**4**	

Standard Form 298 (Rev. 8-98)
Prescribed by ANSI Std Z39-18

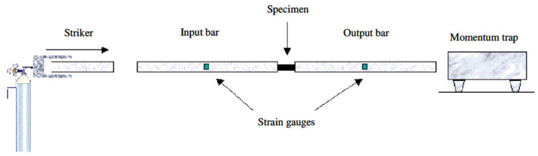

Fig. 1. Representation of a Split Hopkinson bar.

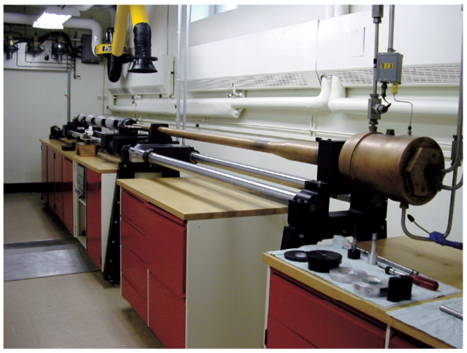

Fig. 2. View of the experimental setup.

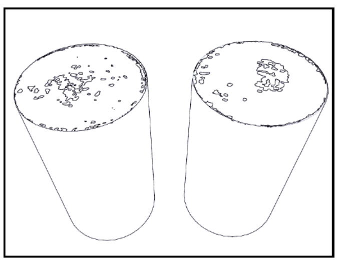

Fig. 3. An amplification view of the damage observed on the input (right) and output (left) bars.

consists of a gas gun that propels a steel striker bar. The striker diameter and length used for this test series are respectively, 14.3 mm and 200 mm. The input and output bars both have a diameter of 14.5 mm, a length of 800 mm and are both made from maraging steel. The sound speed and impedance of the maraging bars were measured experimentally and they are respectively equal to 4750 m/s and 6325 kg/s. The photograph shown in Figure 2 gives a view of the experimental test set-up viewed from the incident bar end.

During a test series on a brittle material, the surfaces of the bars at the sample/bars interface were damaged. Specimens from the brittle material tested have broken apart and produced indentations at the bars surface and an evaluation of the surface condition was done using a DEA Bridge Gamma 1203 scanner. The accuracy of the reading was within 9.0 μm ($\pm$4.5 μm) in the x, y and z directions. Figure 3 shows the damage on the surfaces which is mostly located in the middle and at the edge of the surfaces. The maximum measured variation in material indentation was 100 μm.

After the damage was confirmed and measured, the well characterized Al 6061-T6 was used to verify if rough surfaces influence the signal response and thus the data collected. The Aluminum specimen tested was 10.5 mm in diameter and 5 mm in length. The controlled tests were

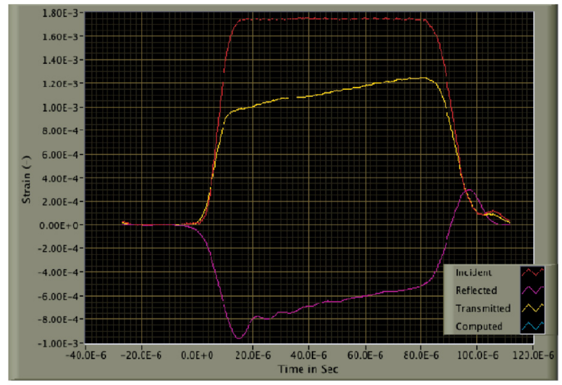

Fig. 4. Aluminium Al 6061-T6 tested with undamaged bars.

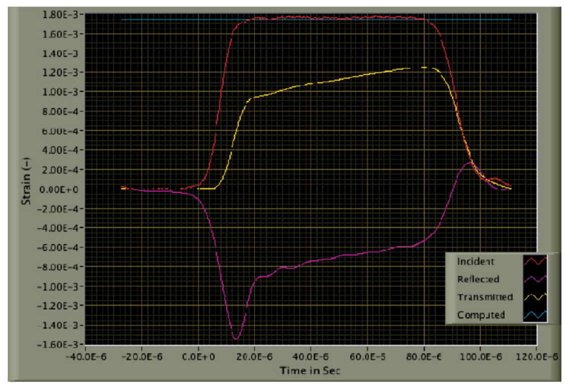

Fig. 5. Aluminium Al 6061-T6 tested with damaged bars.

conducted using a striker that had an impact velocity equal to 16.8 m/s. Figures 4 and 5 give the strain as a function of time for the tests conducted using undamaged and damaged bars. The incident strain computed on the input bar (red curves) had a maximum equal to 1.8 E^{-3} in both experimental setups. This equality is obvious since the incident data (e.g. stress, strain) are not influenced by end-surface conditions. In the opposite, the strain associated to the reflected wave collected using damaged surfaces (pink curves) was significant ($1.55\,10^{-3}$) when it compared to that of undamaged bars ($0.95\,10^{-3}$).

Assuming that the specimen deforms uniformly, the strain within the specimen is directly proportional to the amplitude of the reflected wave, and the stress is directly proportional to the amplitude of the transmitted wave. Therefore, Equation (3) can be used to compute the strain in the specimen. In Equation (3), l_0 is the specimen length prior to impact.

$$\varepsilon_s(t) = -\frac{2c}{l_0}\int_0^t \varepsilon_r(t)dt \tag{3}$$

Using Equation (3), strain in the Aluminum specimen tested with the two setups were computed and plotted in Figure 6. It shows clearly the effect of damage on the computed amplitude of the true strain in the sample. Using damaged bars, there is a significant increase of about 20% in the maximum strain obtained.

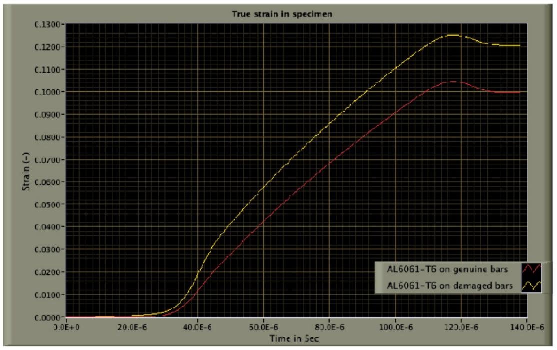

Fig. 6. Computed true strain in the specimen in both bar conditions.

To understand and isolate the effect of surface damage on bar response, the approach used consists of introducing series of known gaps between a non-damaged input and output bars to simulate a variation of surface damage. In this series of tests there were no specimens between the two undamaged bars. In parallel, numerical simulations were performed using a hydrocode to confirm that signal response could not be associated with several types of error in the system. The approach used for numerical simulations is presented in the following section.

4 Numerical modelling

A hydrocode is a finite element algorithm for the modelling of large deformation at all speeds in mechanics of continuous media. Therefore, it can be used to treat various rheological models of material behaviour at high strain rates. They can be based on either Lagrangian or Eulerian formulation. In this study, the LS-Dyna hydrocode was used to investigate the possibility of numerically modelling wave propagation in split Hopkinson bar and the effect end-surface damage on the data collected.

The mesh generated for the Hopkinson bar took advantage of the axisymmetric nature of the simulation and thus only half of the problem was modeled. Therefore, a two-dimensional simulation and four-node quadrilateral elements were used throughout of the model. A special consideration had been taken when meshing the input and output bars as may the shape and the size of the elements influence the results [4]. To not loss accuracy during calculation, 0.16-mm-length elements were used to model the bars. Figure 7 shows the finite-element mesh used for the simulations.

Modeling surfaces that have been damaged is not obvious. The approach taken was to space out the two bars with a gap to approach the indentation depth. Because no specimen was modelled and the input and output bars stay in the elastic regime, the kinematic-isotropic elastic-plastic constitutive material model was used to model the bars. This constitutive model implies a bilinear stress/strain curve. The bars and striker materials were made from Maraging steel and their mechanical properties are given in Table 1.

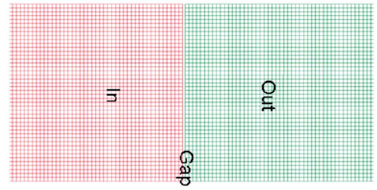

Fig. 7. The input and the output bars meshed with quadrilateral elements.

Table 1. Material properties for Maraging Steel.

Physical Parameters	Maraging Steel
Density (kg/m^3)	8064
Yield Strength (Pa)	965 10^6
Elastic Modulus (Pa)	182 10^9
Poisson's Ratio	0.3
Tangent Modulus (Pa)	1.73 10^9

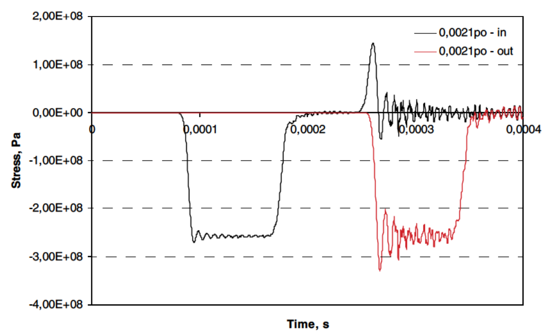

Fig. 8. Incident and transmitted axial stress, $V_{striker} = 13.6$ m/s, Gap $= 53.3\,\mu$m (0.0021 inch).

In the case of Maraging steel, the density and the elastic modulus of bars were measured experimentally. In all the simulations, a perfect contact between the bars was assumed and the frictional forces were ignored.

5 Results and discussion

Figure 8 shows axial stress as a function of time for a striker velocity equal to 13.6 m/s and a gap of 53.3 μm (0.0021 inch). Upon impacting the input bar, the striker generated a compressive wave that travelled along the input bar. In the case shown below, the incident and the transmitted signals are given at the centre of each bar. After 8.4 μs from the time impact, the compressive wave arrives at the middle of the input bar. The amplitude of the compressive wave in the input bar reaches an average value of 258 MPa. At 25.4 μs, a fraction of the wave is reflected at the input-bar free surface as a tensile wave. If the two bars were in a perfect contact, the entire compressive wave would be transmitted to the output bar and none would be reflected given that the two bars are made from the same material.

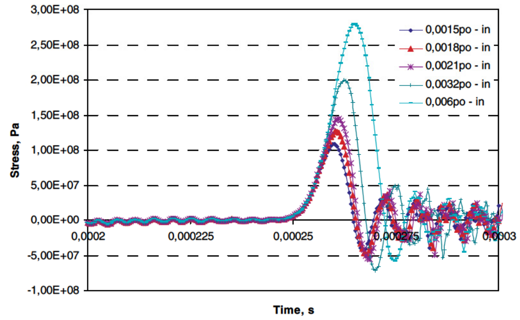

Fig. 9. Tensile wave in the input bar for different gaps (given in inch), $V_{striker} = 13.6$ m/s.

Due to the gap between the two bars, the input bar took 15.6 μs to reach the output bar. The average stress transmitted to the output bar is the same as the one in the input bar (258 MPa) but due to the gap between the two bars, the duration of the transmitted wave was shorter than the incident wave. The duration of the incident wave is 88.7 μs and in the output bar is 85.7 μs. The difference between the two durations corresponds to the duration of the tensile wave in the input bar. In fact, the reflected tensile wave travelling through the input bar generated a stress amplitude equal to 143 MPa with a duration equal to 3.2 μs.

Figure 9 shows the tensile stress-time histories using different gaps. The magnitude and duration of these waves increase with the gap distance. The time delay is the duration that the input bar took to reach the output bar and can be calculated analytically by dividing the corresponding gap by the particle velocity of the bars. This approach may be useful when the condition of the bars is unknown.

In parallel, experimental tests were performed to verify that the introduction of a gap comparable to the mean surface damage variation is a valid approach. The case discussed in this paper was for a gap of approximately 150 μm (0.006 inch) and a striker velocity of 16.8 m/s. Two cases were tested with these conditions, one for damaged surface with an Al 6061-T6 sample and no gap and another with highly polished surface but with a 150 μm gap. The duration of the tensile wave in the input bar was equal to 11.5 μs the case of highly polished surfaces. In the other case, the duration of the tensile wave was approximately of the same amplitude (9.5 μs). Also, and as expected, the incident and transmitted strain have the same amplitude for the tests with no specimen. Using the same conditions in the numerical simulations for the gap and striker velocity and no specimen, the duration of the tensile wave was 11.8 μs which is in good agreement with the experimental test.

6 Conclusion

Control tests were conducted using Al 6061-T6 samples to investigate if surface damage at the interface between the sample and the bars of a split Hopkinson bar test setup influences the sample response and strain data acquired. Results showed that artefacts were introduced into the signal due to damage on the interface surfaces. The method of using extremely small gaps at the interface to simulate interface surface damage was presented. This method was used to confirm and quantify interface surface damage and its induced errors using both simulations and experiments. The simulations corroborate the fact that artefacts introduced by the interface surface damage were not part of the inherent errors normally accounted for in the test setup. Thus, using the time delay in the tensile wave, end-bar conditions can be quantified and the strain rate data be filtered to remove the artefact introduced by the interface surface damage.

References

1. Kolsky, H., An Investigation of the Mechanical Properties of Materials at Very High Rates of Strain, *Proc. Roy. Phys. Soc.*, **B 62,** pp. 676-700 (1949)
2. Bolduc, M., *Split Hopkinson bar experiment: Aluminum 6061-T6,* Technical Memorandum, DRDC Valcartier TR 2004-362, (2006).
3. Kaiser, M.A. *Advancements in the Split Hopkinson Bar Test.* Thesis in Mechanical Engineering. Blacksburg, Virginia. (1998).
4. Bouamoul. A., *2D Hopkinson bar simulation analysis: Al 6061-T6 specimens,* Technical Memorandum, DRDC Valcartier TR 2004-363, (2005).
5. Bolduc, M and Arsenault, R. *Improving Accuracy in SHPB,* Technical Report, DRDC Valcartier TR 2005-380, (2005).